PLOS ONE

RESEARCH ARTICLE

Synthesis of length-tunable DNA carriers for nanopore sensing

Zachary Roelen, Vincent Tabard-Cossa*

Department of Physics, University of Ottawa, Ottawa, Ontario, Canada

* tcossa@uottawa.ca

OPEN ACCESS

Citation: Roelen Z, Tabard-Cossa V (2023) Synthesis of length-tunable DNA carriers for nanopore sensing. PLoS ONE 18(8): e0290559. https://doi.org/10.1371/journal.pone.0290559

Editor: Elingarami Sauli, Nelson Mandela African Institute of Science and Technology, UNITED REPUBLIC OF TANZANIA

Received: July 12, 2023

Accepted: August 9, 2023

Published: August 23, 2023

Data Availability Statement: All relevant data are within the manuscript and its Supporting Information files.

Funding: This work was supported by the Natural Sciences and Engineering Research Council of Canada (NSERC), through funding from grant #CRDPJ 530554-18, and the National Institutes of Health, through funding from grant R01 EB031581. The funders had no role in study design, data collection and analysis, decision to publish, or preparation of the manuscript.

Abstract

Molecular carriers represent an increasingly common strategy in the field of nanopore sensing to use secondary molecules to selectively report on the presence of target analytes in solution, allowing for sensitive assays of otherwise hard-to-detect molecules such as small, weakly-charged proteins. However, existing carrier designs can often introduce drawbacks to nanopore experiments including higher levels of cost/complexity and carrier-pore interactions that lead to ambiguous signals and elevated clogging rates. In this work, we present a simple method of carrier production based on sticky-ended DNA molecules that emphasizes ease-of-synthesis and compatibility with nanopore sensing and analysis. In particular, our method incorporates the ability to flexibly control the length of the DNA carriers produced, enhancing the multiplexing potential of this carrier system through the separable nanopore signals they could generate for distinct targets. A proof-of-concept nanopore experiment is also presented, involving carriers produced by our method with multiple lengths and attached to DNA nanostructure targets, in order to validate the capabilities of the system. As the breadth of applications for nanopore sensors continues to expand, the availability of tools such as those presented here to help translate the outcomes of these applications into robust nanopore signals will be of major importance.

Introduction

Molecular carriers are a sub-category of an increasingly popular trend in nanopore sensing to use designed, structured molecules to characterize a sample of biological interest [1] or to probe the fundamentals of polymer physics [2]. Under the molecular carrier scheme, instead of sensing a target analyte directly with a nanopore, a proxy molecule ("carrier") that interacts with this target (or with intermediate reporters of the target) is sensed [3, 4]. The key requirement of this approach is for the nanopore signals generated by the translocating carriers to be recognizably different depending on whether this interaction with the target has occurred or not. For instance, a target could bind to a specific subregion of a carrier, resulting in this subregion blocking additional ionic current when passing through the pore (as compared to without the target attached) [5]. In this way, the presence of the target analyte can be observed indirectly through its effect on the carrier.

A primary candidate for a carrier molecule is double-stranded DNA (dsDNA), which features high levels of regularly-spaced negative charge along its backbone and which has been extensively characterized inside the nanopore system [6]. In addition to being readily captured

Competing interests: We have read the journal's policy and the authors of this manuscript have the following competing interests: V.T.-C. is CSO of Northern Nanopore Instruments Inc., a for-profit company that provides solid-state nanopore tools and software, including the Nanolyzer software used here. Z.R. declares no conflicts of interest. This does not alter our adherence to PLOS ONE policies on sharing data and materials.

under an applied electric field, the rigid, double-helical structure of dsDNA results in it having a relatively open, extended conformation in solution [7], allowing for positional information (such as the attachment of a target molecule along its contour) to be read out in its translocation signal as it threads sequentially though the pore. To build a molecular carrier based on DNA, commercially-produced viral genomes are often used as the starting point [8–16]. These have the advantages of being widely available and of possessing known sequences around which their target-selective functionalities can be designed.

While molecular carriers produced from viral genomes can be versatile, there are some downsides associated with such sources of DNA. For one, an extended genome, such as the commonly used λ (48.5 kbp) [15, 16], represents a long length for a nanopore analyte (typically $\lesssim$ 10 kbp [6, 17, 18]). The longer a DNA molecule is, the more prone it is to entering the nanopore in a folded conformation [19, 20] which could the cause the local, intra-event signals generated by substructures in the molecule (e.g. as from attached targets) to be read outside of their expected order [13, 21]. Greater proportions of events going unrecognized in this way can necessitate longer experiment times (to generate sufficient statistics from the non-rejected events) and may even lead to experimental bias if correlations exist between the folding frequency of a carrier and its state of target attachment. Longer molecules also tend to irreversibly stall more often during a translocation attempt ("pore clogging"), potentially ending a single-pore experiment early before all sample conditions can be tested.

Additional issues can also arise from sourcing purified versions of these viral templates commercially. While widely available from popular vendors in several molecular configurations and order sizes, these purified genomes may become costly to purchase in the quantities needed to continuously run nanopore experiments, especially if losses are incurred in their subsequent processing into their final, modified forms. There is also variability that can exist (e.g. batch-to-batch, vendor-to-vendor) in the quality of a particular template sample, for instance in the fraction of normally circular genomes (e.g. M13 [8]) that can arrive randomly sheared (and therefore linearized) partway through their sequence. This can translate into experimental variability if, after processing, the defective copies of the molecule present in the sample lead to altered nanopore signals.

The overall goal of this work is therefore to develop a protocol for the in-lab synthesis of DNA carriers that are well-suited for nanopore sensing. In particular, we focus on a design that follows the general structure of λ-DNA, namely, linear, double-stranded molecules that terminate in single-stranded overhangs ("sticky ends") onto which targets may be attached by sequence-specific DNA hybridization. Two main objectives are prioritized when developing the protocol. The first is to have any methods used be achievable with standard, countertop molecular biology lab equipment (e.g. thermocycler, gel electrophoresis system, microcentrifuge). This lowers the barrier for other researchers to make use of and iterate on these methods, without the need to procure access to highly-specialized, institution-shared equipment (e.g. HPLC system, ultracentrifuge). Note, however, that restricting ourselves to these common tools still allows for plenty of flexibility in the design and functionality of the molecular outputs. For instance, the powerful polymerase chain reaction (PCR) technique combines the thermocyler with a handful of widely-available consumables (including a thermostable DNA polymerase) to repeatably amplify DNA fragments with specific targeted sequences and can readily incorporate functional groups or labels into these fragments by simple substitutions in the starting materials (e.g. using modified dNTPs or primers) [22, 23].

The second priority when designing our synthesis protocol is to allow the overall length of the sticky-ended carriers produced through these methods to be highly adjustable. As discussed above, a DNA fragment that is overly long can be problematic for nanopore sensing through its increased tendencies to adopt complex, difficult to analyze conformations and to

clog pores. Conversely, there are also complications to sensing very short DNA fragments, arising from the finite bandwidth of the system used to measure the small nanopore currents (centred around a low-noise amplifier)–short fragments may translocate the membrane too quickly to be reliably detected or to have the details of their signals be well resolved by this system. Beyond the need for an intermediate fragment length between these two extremes however, there is additional utility in the context of molecular carriers to being able to finely adjust the product length within this range. This is because carrier length represents another variable by which carriers mapping to different assay targets could be separated by a nanopore, specifically through the dwell times or equivalent charge deficits of the translocation events they produce [17, 24, 25]. Moreover, many of the techniques previously used for carrier identification (such as barcoding [9, 14] or end-labelling [16]) can be applied simultaneously with length selection on the same molecule, creating a multiplicative effect that supports high levels of multiplexing from a small number of variants in each mode.

In this work, we present a method for synthesizing sticky-ended DNA molecules (SE-DNA) that adheres to the objectives outlined above. The basic protocol is first outlined, with key aspects to its design highlighted that allow for the length of the product and the sequence of its sticky ends to be adjusted, as well as for compatibility with nanopore sensors to be maintained. Following on this, the capabilities of molecules produced by this method as molecular carriers are validated with a proof-of-concept nanopore experiment.

Results and discussion

Method outline

A schematic of the overall synthesis process of sticky-ended DNA molecules (SE-DNA) is presented in Fig 1A. It begins by selecting a DNA template with a known sequence (e.g. from a commercially-sourced bacteriophage genome) such that PCR primers can be designed to amplify a specific internal subregion of this sequence. After amplification, the product is digested with restriction endonucleases to create short (e.g. 4 nt) single-stranded overhangs on one or both ends of a central fragment. These ssDNA overhangs are targeted in a subsequent ligation step as the attachment sites of small double-stranded "linker" molecules.

The specific design of the linkers used in this step will define both the presence and the sequence of the sticky ends of the final product. In the example presented in Fig 1A, the PCR amplicon has been digested by two restriction enzymes to produce a different short ssDNA overhang on each end. The linker in this example then consists of two oligonucleotides, each of which features a complementary region to one of the two short overhang sequences (red and green segments in Fig 1A) followed by a region that is complementary to its analogue on the other linker strand, allowing for their hybridization into a single molecule. In this case, the sticky end sequences on the final product will be the same as those holding the two linker strands together, and will thus be cohesive with each other. However, by choosing to use one or two different linker molecules (two or four linker oligonucleotides) and by varying the lengths and specific sequences of their central regions, an essentially arbitrary ssDNA extension could be independently placed on one or both ends of the final product.

The final step in the process consists of melting off one of the linker strands on each end to expose the desired ssDNA extensions comprising the sticky ends. This relies on the fact that the linker molecules are not 5′-phosphorylated (as can be specified when ordering commercial chemically-synthesized DNA oligos) and so during the ligation step, only their 3′ ends are covalently attached to the digested amplicon by the ligase. This leaves nicks placed near the ends of the products that lead to relatively unstable terminal stretches of annealed dsDNA (~10 bases long, exact length determined by the linker sequences, see Fig 1A) that can be

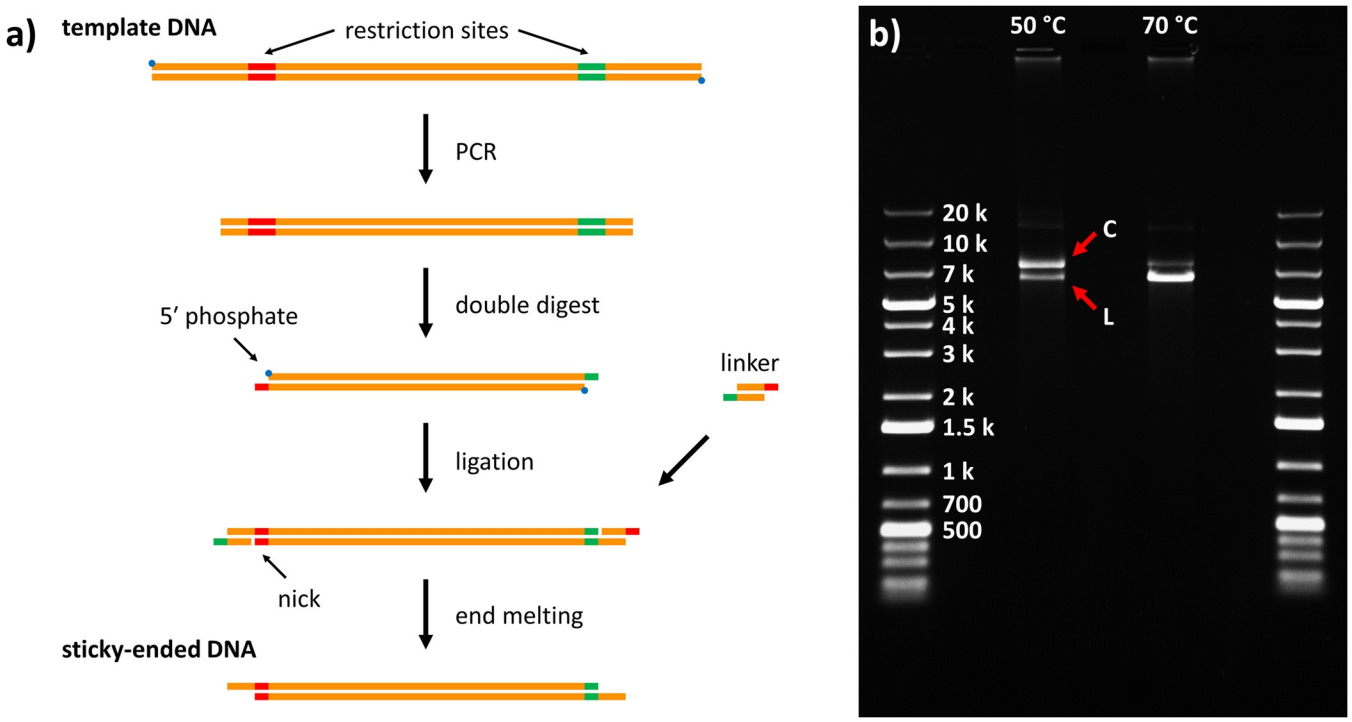

Fig 1. Method outline. a) Overview of the basic SE-DNA synthesis protocol. The length of the final product is determined primarily by the distance between the two restriction sites (which can be adjusted as desired during the PCR step, see main text) while the number of sticky ends and their sequences are flexibly determined by the choice of linker molecule(s). **b)** Agarose gel (0.5%, 0.5× TAE, pre-stained with Gel Red, 70 V) of 6.2 kbp SE-DNA produced by this method, here using λ-DNA template, KpnI and SacI restriction enzymes, and a single linker. The second lane from the left ("50˚C") is the result of incubating the product for 1 hr at 50˚C (~1 nM DNA in 10 mM $MgCl_2$) and shows two main bands: the linear product ("L") migrating between the 5 kbp and 7 kbp DNA ladder bands, and a slower-migrating circular product ("C") resulting from the annealing of the two complementary ends of a linear molecule. The next lane over ("70˚C") is the result of taking an aliquot of the same "50˚C" mixture and heating it above the melting temperature of the 12-nt sticky ends (10 min at 70˚C)–here the circular band is greatly reduced in favour of the linear band as the annealed ends of the circles are reversibly melted.

https://doi.org/10.1371/journal.pone.0290559.g001

selectively melted by heat or chemical denaturation, leaving the stable central region that composes the bulk of the molecule (~1000+ bases long) intact. S1 and S2 Files in the Supporting Information contain the oligo sequences used in this work (primers and linkers), as well as detailed experimental protocols, respectively.

Referring back to the example of 1A we see that the length of the final sticky-ended product in this case is determined primarily by the distance between the recognition sites of the two restriction enzymes in its blunt precursor (PCR amplicon). An obvious method of modifying this length to meet the needs of an application could therefore be to target alternative recognition sites in the template sequence or even to use different restriction enzymes. There are, however, several downsides to such an approach. For one, the exact product lengths achievable this way are limited to only those that correspond to the locations of existing recognition sites (which may or may not be beneficially distributed in a given DNA template). Additionally, using different restriction enzymes on a template typically produces different cleaved ends, varying in overhang length (including 0 nt–blunt ends), polarity (5′ or 3′), and/or sequence. This necessitates careful consideration that a targeted cleavage site is compatible with the construction of a particular product, or, at the very least, requires the re-design and purchase of additional linker molecules for each new cut type.

A more flexible approach to setting the product length might instead start with the selection of a single set of restriction enzymes whose recognition sites are rare or non-existent in the native sequence of the DNA template. New recognition sites for these enzymes can then be

introduced at practically arbitrary locations within the template (thus defining the product length) by modification of the primers used in the PCR stage of synthesis–either by point mismatches between primer and template to create cleavage sites from closely-related sequences or by simple addition of the recognition sequence (typically ~6 bp) to the 5′ end of the primer [26]. S3 File in the Supporting Information presents an illustrative example involving the combination of KpnI and SacI restriction enzymes with a λ-DNA template, where the "forward" PCR primer is fixed near the location of a KpnI site and the "reverse" primer is placed somewhere within the region directly downstream (~17 kbp wide), which is devoid of SacI sites in native λ-DNA. Even when restricting the placement of the reverse primer to sequences within this region that differ by one base at most from a SacI site (and so could be converted to an active site with a single base substitution in the primer), a full range of product lengths from 0–17 kbp is achieved, with an average gap between adjacent lengths of ~350 bp (see S3 File). Creating a wide range of different SE-DNA product sizes in this case then involves modifying a base synthesis protocol by only a single, low-cost PCR primer at a time.

Finally, we note the importance of removing any "extra" DNA fragments with single-stranded overhangs that appear at various stages of the synthesis protocol. These include the "caps" of the PCR amplicon that are cleaved off of the central fragment during the restriction digest, as well as any excess linker molecules that have not been incorporated onto this fragment during the ligation stage. If these spurious fragments are not removed, their presence in the reaction mixtures of subsequent stages could create interference by annealing with complementary regions on the main product and thus blocking interactions of these regions with their intended targets (see Fig 1A). So long as these extra fragments were relatively short ($\lesssim$ 100 bp), their separation from the larger (1000+ kbp) main product was found to be easily achieved by incorporating a standard DNA purification step–e.g. by silica membrane-based spin column or alcohol precipitation–in between synthesis stages (see S4 File in the Supporting Information). Crucially however, it was observed that any purification attempts that involved extracting DNA from agarose gels (as might be necessary for separating larger DNA fragments by size) created problems for the downstream nanopore sensing of these molecules. We found that samples that had interacted with agarose systematically led to increased pore clogging (both reversible and irreversible with voltage inversion or solution flushing) and additional, low-amplitude blockages in the current signal (as if from contaminants), when compared to control samples that lacked agarose purification (see S5 File). It is therefore important to design any intermediate regions that will not make it into the final product (such as between a restriction site and the end of a PCR amplicon) to be relatively short and thus easily separable.

Fig 1B shows a gel image of a 6216-bp product created with the above protocol (using a λ-DNA template and KpnI/SacI restriction enzymes) that features two (5′, 12-nt long) cohesive ends, as in the example of Fig 1A. The first output lane (labelled "50˚C") shows the result of incubating a sample of this product at intermediate temperatures (50˚C), below the melting point of the sticky ends, for 1 hr (~1 nM DNA in 10 mM $MgCl_2$ + 10 mM Tris, pH 8). Two main populations are visible–a faster band migrating between the 5- and 7-kbp bands of the ladder that is attributed to the linear 6.2 kbp product, as well as a slightly slower-migrating band that is attributed to the two cohesive ends of the product annealing to form a circular molecule. A third, slower band is faintly visible above these two (between the 10- and 20-kbp bands of the ladder) and may represent rare dimers that were formed during the ligation step. In the adjacent output lane ("70˚C"), an aliquot of this same sample mixture was briefly heated at temperatures above the melting point of the 12-nt ends (10 min at 70˚C) and then immediately submerged in an ice bath. In this case, the "circular" band is greatly reduced in favour of the "linear" band, confirming that the sample contained at least a substantial proportion of products with two active sticky ends–ends that were stably annealed to each other at

intermediate temperatures and that could be reversibly dissociated (not locked-in during the ligation stage) with simple temperature cycling, as desired.

Validation

To test the viability of sticky-ended DNA produced by these methods to act as molecular carriers in a nanopore experiment, two product lengths were constructed (1842 bp and 6216 bp) that shared a λ-DNA template, KpnI and SacI restriction enzymes, and a single linker molecule, but that differed in their PCR primers, as outlined in the previous section. The particular linker used here resulted in two complementary ssDNA extensions (5′, 12 nt long) being created on either end of each product–see S1 File in the Supporting Information for the exact oligo sequences (PCR primers and linkers) used.

As proof-of-concept carrier targets, DNA multi-way junctions were utilized in this work. These DNA nanostructures have previously been demonstrated to generate recognizable translocation signals on a nanopore [14, 27, 28]. Here, 12-way junctions ("12-arm stars") were designed such that each junction arm was 24-bases long, with one of the arms featuring a 12-nt single-stranded extension that is complementary in sequence to a sticky end on the carrier. Incubating a sample of carriers with an excess ($\gtrsim 30\times$) of complementary DNA stars then resulted in the majority of carrier molecules having a target star attached to one end (see S6 File for an example gel shift assay of this attachment step).

A schematic of the nanopore set-up used to detect these carrier-target constructs is illustrated in Fig 2A. Under this scheme, a DNA sample is first diluted in a high-ionic strength buffer (3.6 M LiCl, pH 8) and injected on one side of the pore-containing membrane. A voltage applied across the membrane is then used to transport the negatively-charged molecules though the pore by electrophoresis. As individual molecules approach and translocate though the pore, they block portions of a background flow of ions (Li^+ and Cl^- in this case) that are also being electrophoretically driven across the membrane. Molecular translocations can thus be detected with high-bandwidth amplifiers through the transient current fluctuations ("events") they create, signalling the presence of the target molecules in a sample and allowing for their characterization through the details of their current signatures [3, 29].

Fig 2B shows a sample current trace of such a translocation event (here resulting from a 12-arm star attached to a 1.8-kbp carrier and passing through a ~13-nm pore), where the amount of ionic current being blocked over time is displayed. Overlaid on top of the raw blockage values (in grey) are a set of fitted step functions ("sublevels") that relate to different substructures of the molecule passing sequentially through the pore [30, 31]. In this case, the sequence consists of a baseline (open pore) sublevel, followed by two relatively shallow and long-lived sublevels (corresponding to the extended DNA carrier), then two relatively deep and short-lived sublevels (corresponding to the bulky DNA star), and finally a return to baseline. This suggests that this particular structured molecule was initially captured by its carrier end (specifically in a hairpin configuration given the blockage depth of the first level being ~double that of the second [6, 32]) which then threaded through the pore until the bulkier DNA star was reached, resulting in elevated blockage levels above those of the carrier.

Two analysis metrics were employed here to characterize the nanopore signals generated by translocating carrier/DNA star molecules–"max deviation" and "truncated ECD". Max deviation corresponds to the single point of deepest blockage in the signal and is calculated as the difference (in current) between this point and the averaged baseline values (see Fig 2B). As discussed, for hybridized carrier-target molecules, the point of deepest blockage is expected to occur during the translocation of the bulky star attachment and so max deviation indirectly characterizes its size through how much current is blocked [33]. Truncated ECD (for

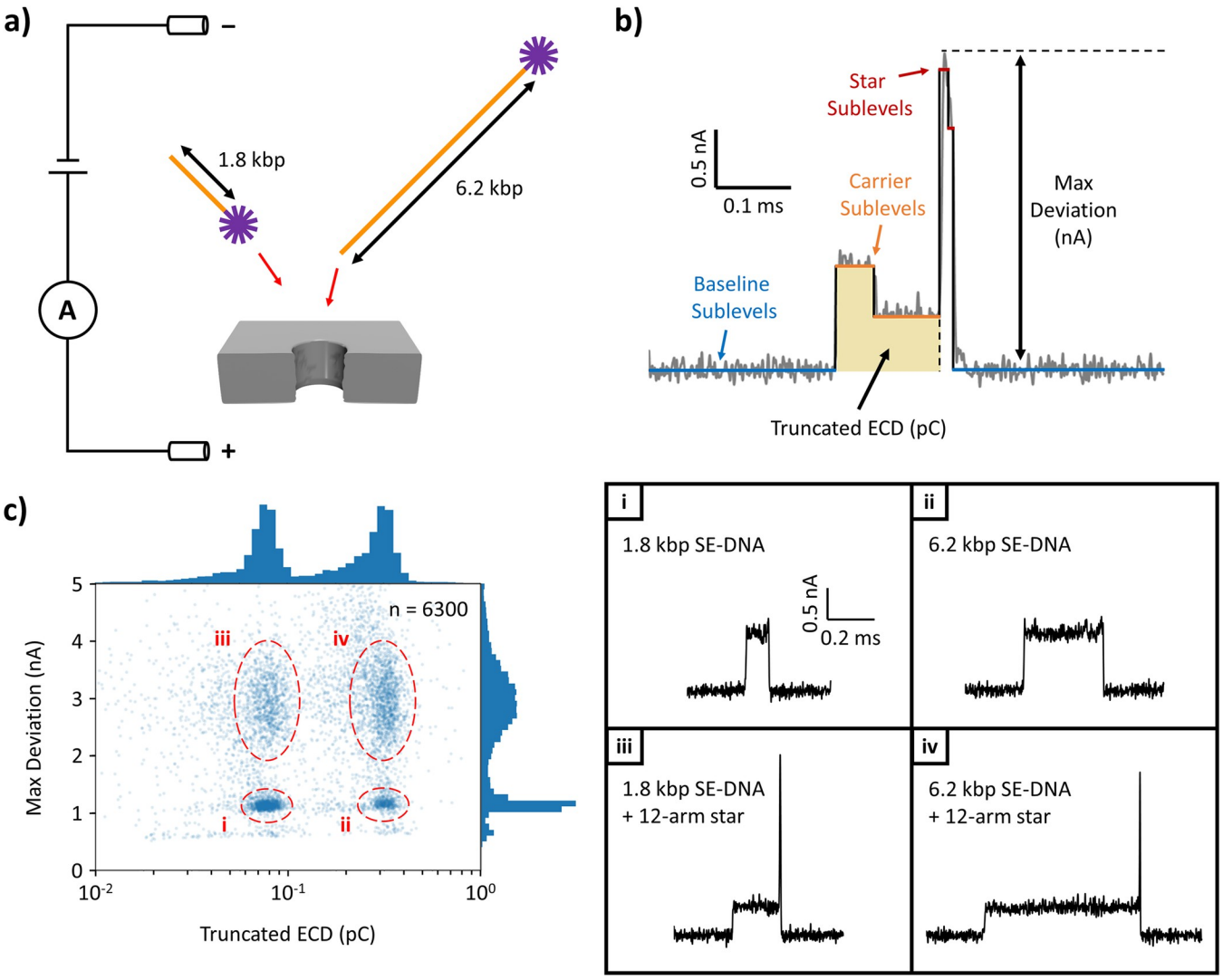

Fig 2. Validation. a) Schematic of the experimental set-up for nanopore detection of a DNA nanostructure attached to multiple SE-DNA lengths. 1.8 kbp and 6.2 kbp SE-DNA molecules were first combined with 12-arm DNA stars via the hybridization of complementary single-stranded extensions from each piece. Individual (negatively-charged) hybrid DNA structures were then electrophoretically driven through a nanopore, generating transient fluctuations ("events") in a background ionic current while they obstruct the pore. **b)** Sample translocation event (current blockage vs. time) illustrating calculations of the event statistics "max deviation" and "truncated ECD" (TrECD). **c)** Scatter plot of max deviation vs. log[TrECD] for events from a single nanopore experiment (~13 nm pore diameter, 3.6 M LiCl pH 8 buffer, 150 mV transmembrane potential). Two main peaks are visible in the histograms (along the margins of the scatter plot axes) of both statistics, resulting in four total event populations corresponding to: i) 1.8 kbp SE-DNA on its own, ii) 6.2 kbp SE-DNA on its own, iii) 1.8 kbp SE-DNA attached to a 12-arm star, iv) 6.2 kbp SE-DNA attached to a 12-arm star. Representative current traces of events from each of the four populations are presented in the panels on the right.

https://doi.org/10.1371/journal.pone.0290559.g002

"equivalent charge deficit"), on the other hand, is the integrated area underneath particular fitted sublevels of the event (in between these levels and the baseline) [21]. Here we specifically use the levels attributed to blockages of the carrier within the overall event (see Fig 2B), in order to characterize the length of these carrier molecules through how much total charge they block. Under nanopore conditions where DNA folding is permitted, ECD has been previously been demonstrated to be a more reliable measure of DNA length when compared to overall passage time [17, 24, 25], since folded sections of the polymer are more compact and so can pass through the pore in shorter times than their fully-extended analogues (in the absence of pore wall interactions).

Fig 2C shows a scatter plot of max deviation vs. truncated ECD (log-scaled) for all carrier translocation events of the same nanopore experiment as the example of Fig 2B (1.8 kbp and 6.2 kbp carriers incubated with 12-arm stars, run though a ~13 nm pore at 150 mV in 3.6 M LiCl pH 8). Excessively short events in duration (< 40 μs) resulting from unsuccessful translocations ("collisions") or the passage of free DNA stars have been removed prior to plotting to reduce clutter (see S7 File). From either the scatter plot itself or from 1D histograms of each metric plotted on the axis margins, at least four main event populations can be identified that are easily associated with the particular configurations of translocating molecules that produced them. The two peaks in truncated ECD, at 77^{+22}_{-17} fC and 312^{+99}_{-75} fC, correspond to the two different carrier lengths of 1.8 kbp and 6.2 kbp present in the sample. Meanwhile, there is a broad peak (2.9 ± 1.0 nA) at higher values of max deviation and a narrow peak (1.1 ± 0.1 nA) at lower max deviations corresponding to carriers with and without attached stars, respectively. The large spread in max deviation for signals with a star subevent is likely a combined effect of the many possible configurations available to the 12 arms of a translocating star as well as of the variable attenuation of these fast subevents due to the limited bandwidth of the system [27, 33]. Together, the event distributions in max deviation and truncated ECD combine to create four main populations in the scatter plot corresponding to: i) free 1.8 kbp carriers, ii) free 6.2 kbp carriers, iii) star-attached 1.8 kbp carriers, and iv) star-attached 6.2 kbp carriers. A representative current trace from each population is presented in the rightmost panels of Fig 2C.

By examining the relative numbers of events in each of the populations (separated using statistic thresholds, see S7 and S8 Files in the Supporting Information), a few observations can be made. First of all, there are similar numbers of events resulting from 1.8 kbp (3209 events, populations *i* & *iii*) and 6.2 kbp (3061 events, populations *ii* & *iv*) carriers. This reflects the roughly equal concentrations of both carrier types (~0.4 nM each, as estimated by gel electrophoresis) present in the sample mix introduced to the nanopore. Moreover, within a single carrier type, a majority of events have max deviation values consistent with the attachment of a target star, although the exact ratios differed in the two cases– 58% target-attached (*iii*) / 42% free carriers (*i*) for 1.8 kbp and 79% target-attached (*iv*) / 21% free carriers (*ii*) for 6.2 kbp. This discrepancy between carrier lengths could result from the particular (and arbitrary) choice of sticky ends used here, specifically each molecule containing a set of cohesive ends that can anneal to each other to form a closed circle. The shorter the contour length of a carrier molecule, the more often these two ends will encounter each other in the random conformations they adopt before a target star can be attached, leading to an elevated proportion of shorter length carriers that are bound in a circular state [34]. Indeed, looking at the current traces of individual events from the free carrier populations (e.g. see panels *i* and *ii* on the right of Fig 2C), a large fraction contain only a single blockage level at twice the depth of unfolded DNA, consistent with circularized molecules which can only pass through the pore in an even number of dsDNA fragments (see also S8 File for histograms of average blockage for each population). We note however, that whether this circularization effect is viewed as beneficial or detrimental depends on the specific design and goals of a particular nanopore experiment involving these sticky-ended molecules, and that carriers can easily be constructed with only one sticky end or with two ends of non-complementary sequences using the synthesis methods presented here if circularization is to be avoided.

Conclusion

In summary, a method for the *in vitro* production of sticky-ended DNA was presented for use with nanopore sensing experiments. During the protocol design process, emphasis was placed

on the capacity to synthesize products of variable lengths and the ability to carry out individual protocol steps with common molecular biology equipment and widely-available reagents. Our method was successful in producing molecules that generate robust, easy-to-interpret nanopore signals (Fig 2) by virtue of being linear, double-stranded DNA at their cores (whose translocations have been thoroughly studied in the past) and which feature single-stranded ends through which application-specific functionality can be integrated. Moreover, the 12-nt length of the particular set of (cohesive) ends tested here was observed to represent an good balance of creating stable hybridized constructs under standard nanopore sensing conditions (e.g. temperature, buffer composition) while also offering the ability to quickly dissociate these constructs and re-set the system simply by moderate cycling of the temperature (Fig 1B). Lastly, our protocol was designed to be relatively cost- and time-effective when compared to alternative approaches to DNA carrier production. For instance, in contrast to the DNA origami-like approaches of others [1, 8, 35], which require the purchasing and pipetting of on the order of ~100 oligonucleotide species, the methods presented here make use of a substantially reduced set of reagents, and where only minimal changes to these reagents are needed to make particular product modifications (e.g. replacing a single primer to create a range of product lengths, as in S3 File). Additionally, after using a viral template for an initial run-though, DNA substrates can thereafter be produced in-house by PCR amplification with our protocol, eliminating the need to continuously purchase commercial stocks of DNA.

In the future, the core methods presented here can also easily be adapted through the incorporation of modified dNTPs or oligos [22, 23] during carrier synthesis to meet the needs of future applications that require specific functional groups along their length. The flexibility to integrate further functionality into these molecules post-assembly also exists through the ssDNA overhangs on their ends–these could, for instance, be used as attachment sites for molecular barcodes [9, 14] to more easily distinguish carriers probing for different targets and therefore expand the capability of the system to multiplex. Finally, although molecular carriers have been the focus of this current work, we note that sticky-ended DNA, as a basic construct, may have wider applications to nanopore sensing beyond this. For instance, individual DNA monomers could be chained together by their sticky ends (e.g. circularization, concatemerization [36, 37]) to produce nanopore targets with lengths and structures suited for a particular application, starting from more easily-synthesized (shorter, linear) building blocks. Having a greater number of molecular tools available in this way should only assist in opening new avenues for nanopore sensor research into the future.

Materials and methods

DNA synthesis

DNA carriers were synthesized as described in the main text (detailed protocols are presented in S2 File). Summarizing, a subsection of a DNA template (λ-DNA, New England Biolabs) was amplified by PCR (LongAmp polymerase, NEB) using specific primer oligonucleotides (Integrated DNA Technologies) to define the amplicon length. The PCR output was then digested by restriction enzymes (KpnI and SacI, NEB) to produce a central fragment with single-stranded overhangs. Finally, DNA linker oligos (IDT) were ligated (T4 ligase, Thermo Scientific) to the ends of this central fragment via its overhangs to create new single-stranded extensions defined by the linker sequences.

For the DNA multiway junctions ("stars") used as targets for the carriers, these were assembled from individual oligonucleotide strands (IDT), as described previously [27, 28]. Briefly, a number of strands matching the number of arms in the final structure were mixed in equimolar ratios, heated to 95˚C, and slowly cooled back to room temperature. The sequences of each

strand (48 nt long) are designed to hybridize under these conditions to those of neighbouring strands across two adjacent dsDNA arms (24 bp each). One of the assembled arms is also designed to have a single-stranded extension through which it can be annealed to a complementary extension of the carrier. After assembly, the structures were imaged by polyacrylamide gel electrophoresis, their main gel bands excised, and the purified products resuspended in solution by electroelution (D-Tube Dialyzer Maxi, EMD Millipore).

Nanopore sensing

Nanopores used in this work were fabricated by the controlled breakdown method (CBD), using previously published protocols [38, 39]. In short, a silicon nitride membrane (#NBPX5004Z-HR, Norcada) is immersed in an electrolyte solution (1 M KCl, pH 8) and a relatively large time-varying voltage (~10 V) is applied across it via Ag/AgCl electrodes, using custom instruments and flow cells similar to products from Northern Nanopore Instruments. A computer-controlled amplifier circuit is used to monitor the current through the membrane and to shut off the applied voltage when a sharp increase in this current is detected, signalling the breakdown of the membrane in a single nm-scale hole, as described in Waugh et al. [39].

Prior to a nanopore sensing experiment, a sample of DNA carriers is incubated with an excess of targets (e.g. ~1.5 nM carriers to ~50 nM stars) to anneal the two pieces together (see S6 File). This annealed mixture is then equilibrated with a high-conductivity sensing solution (3.6 M LiCl, pH 8) and 40 μL injected (at a final carrier concentration of ~0.4 nM) on one side of a nanopore-containing membrane (embedded in a flow cell with freshly-flushed 3.6 M LiCl), where an application of moderate transmembrane potentials (~0.1 V) electrophoretically drives the negatively-charged carrier-target molecules through the pore. A high bandwidth current amplifier (VC100, Chimera Instruments), operating at 1 MHz instrument bandwidth (4.17 MHz sampling rate), is used to detect these molecular translocations as fluctuations in the ionic pore current.

Analysis of the current signals ("events") generated by translocating molecules is carried out in the Nanolyzer software package (Northern Nanopore Instruments), which applies a digital low-pass filter to the current trace (400 kHz in this work), locates the events within the timecourse, and fits their signals to step functions that characterize the event substructure (see Fig 2B) [30, 31]. Statistics of the analyzed events (e.g. max deviation, average blockage, dwell time, truncated ECD) were calculated either in Nanolyzer itself, or with custom scripts written in Python using the 'pandas' library.

Supporting information

S1 File. Oligonucleotide sequences.
(PDF)

S2 File. Detailed SE-DNA synthesis protocols.
(PDF)

S3 File. Sample distribution of product lengths.
(PDF)

S4 File. Agarose gels of short fragment removal.
(PDF)

S5 File. Nanopore sensing of agarose-extracted DNA.
(PDF)

S6 File. Agarose gel of carrier/DNA star hybridization.
(PDF)

S7 File. Filtering out short-lived nanopore events.
(PDF)

S8 File. Average blockages of Fig 2 populations.
(PDF)

S9 File. Raw gel images.
(PDF)

Acknowledgments

Z.R. would like to thank Liqun He for help in the design of the protocol to purify DNA multi-way junctions, and Kyle Briggs for advice on nanopore event analysis.

Author Contributions

Conceptualization: Zachary Roelen, Vincent Tabard-Cossa.

Formal analysis: Zachary Roelen.

Funding acquisition: Vincent Tabard-Cossa.

Investigation: Zachary Roelen.

Methodology: Zachary Roelen.

Supervision: Vincent Tabard-Cossa.

Validation: Zachary Roelen.

Visualization: Zachary Roelen.

Writing – original draft: Zachary Roelen.

Writing – review & editing: Vincent Tabard-Cossa.

References

1. Raveendran M, Lee AJ, Sharma R, Wälti C, Actis P. Rational design of DNA nanostructures for single molecule biosensing. Nat Commun. 2020; 11: 4384. https://doi.org/10.1038/s41467-020-18132-1 PMID: 32873796
2. Plesa C, van Loo N, Ketterer P, Dietz H, Dekker C. Velocity of DNA during Translocation through a Solid-State Nanopore. Nano Lett. 2015; 15: 732–737. https://doi.org/10.1021/nl504375c PMID: 25496458
3. Xue L, Yamazaki H, Ren R, Wanunu M, Ivanov AP, Edel JB. Solid-state nanopore sensors. Nat Rev Mater. 2020; 5: 931–951. https://doi.org/10.1038/s41578-020-0229-6
4. Ding T, Yang J, Pan V, Zhao N, Lu Z, Ke Y, et al. DNA nanotechnology assisted nanopore-based analysis. Nucleic Acids Res. 2020; 48: 2791–2806. https://doi.org/10.1093/nar/gkaa095 PMID: 32083656
5. Plesa C, Ruitenberg JW, Witteveen MJ, Dekker C. Detection of Individual Proteins Bound along DNA Using Solid-State Nanopores. Nano Lett. 2015; 15: 3153–3158. https://doi.org/10.1021/acs.nanolett.5b00249 PMID: 25928590
6. Li J, Gershow M, Stein D, Brandin E, Golovchenko JA. DNA molecules and configurations in a solid-state nanopore microscope. Nat Mater. 2003; 2: 611–615. https://doi.org/10.1038/nmat965 PMID: 12942073
7. Kowalczyk SW, Tuijtel MW, Donkers SP, Dekker C. Unraveling Single-Stranded DNA in a Solid-State Nanopore. Nano Lett. 2010; 10: 1414–1420. https://doi.org/10.1021/nl100271c PMID: 20235508

8. Bell NAW, Keyser UF. Specific Protein Detection Using Designed DNA Carriers and Nanopores. J Am Chem Soc. 2015; 137: 2035–2041. https://doi.org/10.1021/ja512521w PMID: 25621373
9. Bell NAW, Keyser UF. Digitally encoded DNA nanostructures for multiplexed, single-molecule protein sensing with nanopores. Nat Nanotechnol. 2016; 11: 645–651. https://doi.org/10.1038/nnano.2016.50 PMID: 27043197
10. Kong J, Bell NAW, Keyser UF. Quantifying Nanomolar Protein Concentrations Using Designed DNA Carriers and Solid-State Nanopores. Nano Lett. 2016; 16: 3557–3562. https://doi.org/10.1021/acs.nanolett.6b00627 PMID: 27121643
11. Kong J, Zhu J, Keyser UF. Single molecule based SNP detection using designed DNA carriers and solid-state nanopores. Chemical Communications. 2017; 53: 436–439. https://doi.org/10.1039/C6CC08621G PMID: 27965988
12. Chen K, Kong J, Zhu J, Ermann N, Predki P, Keyser UF. Digital Data Storage Using DNA Nanostructures and Solid-State Nanopores. Nano Lett. 2019; 19: 1210–1215. https://doi.org/10.1021/acs.nanolett.8b04715 PMID: 30585490
13. Chen K, Zhu J, Bošković F, Keyser UF. Nanopore-Based DNA Hard Drives for Rewritable and Secure Data Storage. Nano Lett. 2020; 20: 3754–3760. https://doi.org/10.1021/acs.nanolett.0c00755 PMID: 32223267
14. Zhu J, Ermann N, Chen K, Keyser UF. Image Encoding Using Multi-Level DNA Barcodes with Nanopore Readout. Small. 2021; 17: 2100711. https://doi.org/10.1002/smll.202100711 PMID: 34133074
15. Sze JYY, Ivanov AP, Cass AEG, Edel JB. Single molecule multiplexed nanopore protein screening in human serum using aptamer modified DNA carriers. Nat Commun. 2017; 8: 1552. https://doi.org/10.1038/s41467-017-01584-3 PMID: 29146902
16. Cai S, Sze JYY, Ivanov AP, Edel JB. Small molecule electro-optical binding assay using nanopores. Nat Commun. 2019; 10: 1797. https://doi.org/10.1038/s41467-019-09476-4 PMID: 30996223
17. Fologea D, Brandin E, Uplinger J, Branton D, Li J. DNA conformation and base number simultaneously determined in a nanopore. Electrophoresis. 2007; 28: 3186–3192. https://doi.org/10.1002/elps.200700047 PMID: 17854121
18. Storm AJ, Storm C, Chen J, Zandbergen H, Joanny J-F, Dekker C. Fast DNA Translocation through a Solid-State Nanopore. Nano Lett. 2005; 5: 1193–1197. https://doi.org/10.1021/nl048030d PMID: 16178209
19. Storm AJ, Chen JH, Zandbergen HW, Dekker C. Translocation of double-strand DNA through a silicon oxide nanopore. Phys Rev E. 2005; 71: 051903. https://doi.org/10.1103/PhysRevE.71.051903 PMID: 16089567
20. Ermann N, Hanikel N, Wang V, Chen K, Weckman NE, Keyser UF. Promoting single-file DNA translocations through nanopores using electro-osmotic flow. J Chem Phys. 2018; 149: 163311. https://doi.org/10.1063/1.5031010 PMID: 30384733
21. Roelen Z, Briggs K, Tabard-Cossa V. Analysis of Nanopore Data: Classification Strategies for an Unbiased Curation of Single-Molecule Events from DNA Nanostructures. ACS Sens. 2023; 8: 2809–2823. https://doi.org/10.1021/acssensors.3c00751 PMID: 37436112
22. Soni G V, Singer A, Yu Z, Sun Y, McNally B, Meller A. Synchronous optical and electrical detection of biomolecules traversing through solid-state nanopores. Review of Scientific Instruments. 2010; 81: 014301. https://doi.org/10.1063/1.3277116 PMID: 20113116
23. Mai DJ, Marciel AB, Sing CE, Schroeder CM. Topology-controlled relaxation dynamics of single branched polymers. ACS Macro Lett. 2015; 4: 446–452. https://doi.org/10.1021/acsmacrolett.5b00140 PMID: 35596311
24. Fologea D, Gershow M, Ledden B, McNabb DS, Golovchenko JA, Li J. Detecting Single Stranded DNA with a Solid State Nanopore. Nano Lett. 2005; 5: 1905–1909. https://doi.org/10.1021/nl051199m PMID: 16218707
25. Bell NAW, Muthukumar M, Keyser UF. Translocation frequency of double-stranded DNA through a solid-state nanopore. Phys Rev E. 2016; 93: 022401. https://doi.org/10.1103/PhysRevE.93.022401 PMID: 26986356
26. Delidow BC. Molecular cloning of PCR fragments with cohesive ends. Mol Biotechnol. 1997; 8: 53–60. https://doi.org/10.1007/BF02762339 PMID: 9327397
27. He L, Karau P, Tabard-Cossa V. Fast capture and multiplexed detection of short multi-arm DNA stars in solid-state nanopores. Nanoscale. 2019; 11: 16342–16350. https://doi.org/10.1039/c9nr04566j PMID: 31386731
28. He L, Tessier DR, Briggs K, Tsangaris M, Charron M, McConnell EM, et al. Digital immunoassay for biomarker concentration quantification using solid-state nanopores. Nat Commun. 2021; 12: 5348. https://doi.org/10.1038/s41467-021-25566-8 PMID: 34504071

29. Ying YL, Hu ZL, Zhang S, Qing Y, Fragasso A, Maglia G, et al. Nanopore-based technologies beyond DNA sequencing. Nat Nanotechnol. 2022; 17: 1136–1146. https://doi.org/10.1038/s41565-022-01193-2 PMID: 36163504

30. Raillon C, Granjon P, Graf M, Steinbock LJ, Radenovic A. Fast and automatic processing of multi-level events in nanopore translocation experiments. Nanoscale. 2012; 4: 4916. https://doi.org/10.1039/c2nr30951c PMID: 22786690

31. Forstater JH, Briggs K, Robertson JWF, Ettedgui J, Marie-Rose O, Vaz C, et al. MOSAIC: A Modular Single-Molecule Analysis Interface for Decoding Multistate Nanopore Data. Anal Chem. 2016; 88: 11900–11907. https://doi.org/10.1021/acs.analchem.6b03725 PMID: 27797501

32. Mihovilovic M, Hagerty N, Stein D. Statistics of DNA Capture by a Solid-State Nanopore. Phys Rev Lett. 2013; 110: 028102. https://doi.org/10.1103/PhysRevLett.110.028102 PMID: 23383940

33. Karau P, Tabard-Cossa V. Capture and Translocation Characteristics of Short Branched DNA Labels in Solid-State Nanopores. ACS Sens. 2018; 3: 1308–1315. https://doi.org/10.1021/acssensors.8b00165 PMID: 29874054

34. Collins FS, Weissman SM. Directional cloning of DNA fragments at a large distance from an initial probe: a circularization method. Proceedings of the National Academy of Sciences. 1984; 81: 6812–6816. https://doi.org/10.1073/pnas.81.21.6812 PMID: 6093122

35. Loh AYY, Burgess CH, Tanase DA, Ferrari G, McLachlan MA, Cass AEG, et al. Electric Single-Molecule Hybridization Detector for Short DNA Fragments. Anal Chem. 2018; 90: 14063–14071. https://doi.org/10.1021/acs.analchem.8b04357 PMID: 30398852

36. Wang L, Meng Z, Martina F, Shao H, Shao F. Fabrication of circular assemblies with DNA tetrahedrons: from static structures to a dynamic rotary motor. Nucleic Acids Res. 2017; 45: 12090–12099. https://doi.org/10.1093/nar/gkx1045 PMID: 29126166

37. Sun L, Åkerman B. Characterization of self-assembled DNA concatemers from synthetic oligonucleotides. Comput Struct Biotechnol J. 2014; 11: 66–72. https://doi.org/10.1016/j.csbj.2014.08.011 PMID: 25379145

38. Kwok H, Briggs K, Tabard-Cossa V. Nanopore fabrication by controlled dielectric breakdown. PLoS One. 2014; 9: e92880. https://doi.org/10.1371/journal.pone.0092880 PMID: 24658537

39. Waugh M, Briggs K, Gunn D, Gibeault M, King S, Ingram Q, et al. Solid-state nanopore fabrication by automated controlled breakdown. Nat Protoc. 2020; 15: 122–143. https://doi.org/10.1038/s41596-019-0255-2 PMID: 31836867